Scientia Iranica C (2022) 29(3), 1364–1376

Sharif University of Technology
Scientia Iranica
Transactions C: Chemistry and Chemical Engineering
http://scientiairanica.sharif.edu

Effect of humic acid on adsorption of methylparaben from aqueous solutions onto commercially available granular activated carbons

A.R. Solaimany Nazar[a,*], M.B. Kurade[b], M. Ali Khan[c], and B.-H. Jeon[b]

a. *Department of Chemical Engineering, University of Isfahan, Isfahan, Iran.*
b. *Department of Earth Resources and Environmental Engineering, Hanyang University, Seoul, South Korea.*
c. *Department of Chemistry, College of Science, King Saud University, Riyadh 11451, Saudi Arabia.*

Received 10 May 2020; received in revised form 4 September 2021; accepted 25 October 2021

KEYWORDS
Humic acid;
Methylparaben;
Adsorption;
F400 GAC;
Norit GAC

Abstract. Adsorption of methylparaben (MP) on Calgon carbon (F400) and Norit-type Granular Activated Carbons (GACs) from aqueous solutions was examined. The influence of Humic Acid (HA) on the adsorption of MP under different pH conditions was evaluated. The adsorption isotherm results are well described by the Freundlich model. The MP adsorption capacity on F400 and Norit GACs was found 150 mg/g. In the presence of Total Organic Carbon (TOC) with 2.357 mg/L HA, the maximum MP adsorption capacity on F400 GAC at pH 7 increased 2.2 folds. The Norit-type GAC had a comparatively higher uptake capacity for MP than F400 GAC. The key mechanism for MP adsorption onto the F400 GAC was through the hydrogen interaction between the -OH functional groups of the MP molecules. The MP adsorption capacity on Norit GAC increased from 5 to 100 mg/g at pH 7.

1. Introduction

Preservatives are organic compounds widely used in food, cosmetics, pharmaceuticals, and personal care products. Because of their wide-range use cases, preservatives constitute a class of Emerging Contaminants (ECs) that are commonly detected in trace amounts (μg/L and ng/L) in surface, sub-surface, coastal, and drinking water [1–3]. Parabens belong to a group of alkyl esters of *p*-hydroxybenzoic acid. They are most commonly consumed as preservatives due to a broad spectrum of their antibacterial activities, acceptable performance in a wide range of pHs, and low cost [4]. Methylparaben (MP) and propylparaben (PP) are the two most frequently used preservatives. The potentially threatening and undesirable effects of parabens on aquatic organisms and human health (estrogenic effects and breast cancer) have become an environmental issue and a major concern worldwide [5–7].

Most of the studies on paraben have assessed their side effects on human health [6,8]. Others have focused on paraben detection, modification, and measurement methods at low concentrations in aquatic environments [9–11]. Lincho et al. [4] reviewed several reported results of the detected parabens in different water sources as well as influent and effluent of sewage treatment plants from different locations worldwide

*. *Corresponding author. Tel.: +98 31 37937027; Fax: +98 31 3793403*
E-mail addresses: asolaimany@eng.ui.ac.ir (A.R. Solaimany Nazar); mayurkurade@hanyang.ac.kr (M.B. Kurade); mokhan@ksu.edu.sa (M. Ali Khan); bhjeon@hanyang.ac.kr (B.-H. Jeon)

doi: 10.24200/sci.2021.55931.4478

with concentrations in the range of ngL^{-1} or greater value around 100 μgL^{-1}. Assessments of paraben removal techniques in wastewater treatment systems indicate that despite parabens degradation, they are still frequently detected in water resources in the range of ng/L concentrations [12]. The average removal efficiency is about 90% for biological treatments; however, the number of parabens absorbed by the process sludge as well as other parabens losses are not reported [5]. A considerable number of parabens are detected in some biological processes in outlet streams [13–15]. Some chlorinated derivatives are produced from the reactions between parabens and the free chlorine ions present in water, which are even more poisonous and resistant to biodegradation than the parent paraben molecules [16]. This secondary chemical production is the main challenge for paraben treatments using the application of advanced oxidation processes [17].

Few studies have addressed the adsorption on paraben. β-cyclodextrin-based polymer was applied to the adsorption of paraben [18]. Amino-modified magnetic nano-adsorbent was tested for the adsorptive removal of parabens attaining up to 98% removal efficiency [19]. Bernal et al. found that π-stacking between basic activated carbon and MP molecule functional groups was the main mechanism governing MP adsorption on activated carbon [20]. The adsorption capacity of MP onto three types of activated carbons was evaluated in terms of textural characteristics and the content of surface phenolic and lactonic groups of activated carbons [21,22]. Equilibrium adsorption experiments of MP and PP using commercial PAC Pulsorb PWX HA pointed to the maximum adsorption capacity in the range of 155 ± 12 mg g^{-1} for both parabens, while in bicomponent experiments, competitive adsorption plays a significant role in reducing the MP adsorption [23]. A major component of naturally occurring dissolved organic carbons is Humic Acid (HA). HAs represent a fraction of humic substances not soluble at a pH lower than 2, but soluble at higher pHs in an aqueous solution [24]. Although coagulation, settling, and sand filtration are the most frequently used drinking water treatment processes, the removal efficiency for Natural Organic Matter (NOM) is limited to within 20 to 50% of typically dissolved humic substances [25]. The Granular Activated Carbon (GAC) based adsorption process is an effective treatment for removing NOM and enhancing drinking water quality [26]. Several studies have evaluated the influence of HA on ECs adsorption behavior onto various types of adsorbents [27–30]. The interaction of HA and ECs and their adsorption mechanisms are not well known and the influence of NOM on paraben adsorption is not well investigated. Simultaneous removal of MP and NOM through the adsorption process requires an experimental assessment to make decisions about the potential treatment applications for water treatment plants.

This study examines the adsorption behavior of MP on Calgon carbon (F400) and Norit-type GACs in HA-containing water to determine an effective treatment method for paraben removal in the presence of NOM in drinking water. These GACs are widely used in many water and wastewater treatment plants and are frequently referred to in the literature as effective adsorbents for the removal of ECs from aqueous media.

2. Materials and methods

2.1. Chemicals, reagents, and GACs

Analytical Reagent (A.R) grade MP with a technical purity of 99.9% was purchased from Sigma-Aldrich, Germany. Solid-powdered commercial-grade HA was procured from Sigma-Aldrich, Switzerland. All other chemicals used during the study were of A.R grade and purchased from Merck, Germany. Two types of commercial GACs viz. Filtrasorb-400 (F400) and Norit PK 1-3 (NPK) were purchased. Filtrasorb-400 is a coal-based steam GAC supplied by Calgon Carbon Asia Pte Ltd. and Norit PK 1-3 (NPK) was produced from peat by Norit Americas Inc. (USA) and purchased from Sigma-Aldrich, Germany. The surface properties of these adsorbents are presented in Table 1. The GACs were rinsed several times with deionized (D.I) water to remove dissolved contaminants and fine particles and then, they were dried at 105°C for 48 h before storage in a desiccator.

2.2. Analytical techniques

The physiochemical properties of the adsorbents are characterized by employing Brunauer-Emmette-Teller (BET) surface area, pore size distribution, Fourier-transform infrared spectrometry (FT-IR), and pH$_{pzc}$ value. The BET surface area analyzer (Microtrac Bel Corp, Model Belsorp mini, Japan) was employed to determine the textural parameters such as surface area

Table 1. GAC BET area and pore volumes.

Adsorbent	S_{BET} (m^2/g)	V_{tot} (cm^3/g)	$V_{supermic}$ (cm^3/g)	$V_{ultramic}$ (cm^3/g)	V_{mic} (cm^3/g)	V_{meso} (cm^3/g)
F400	1,034.0805	0.53809	0.2246	0.100779	0.32467	0.18608
Norit	682.5980	0.37706	0.12106	0.07944	0.2005	0.16248

(S_{BET}), total pore volume (V_{tot}), micropore volume, supermicropore (0.7–2 nm) volume ($V_{supermic}$), ultramicropore (< 0.7 nm) volume ($V_{ultramic}$), and mesopore volume (V_{meso}). The FT-IR spectrometer (Nicolet-Iso50, Thermo Electron, USA) was employed to identify the GACs surface functional groups. The surface morphology of the GACs was observed by a Scanning Electron Microscope (SEM) (Model QUANTA200 ESEM, FEI company, USA). The pH drift method was used to determine the pH_{pzc} of GACs according to the technique presented by Rivera-Utrilla et al. [31].

2.3. MP and HA concentration determination

The MP concentration was measured using High-Pressure Liquid Chromatography (HPLC) and a chromatograph Alliance Water 2695 separations module equipped with a water 2487 UV detector. Aliquots of 100 μL were injected into the HPLC. The isocratic mobile phase was a mixture of 40:60 (v/v) acetonitrile/D.I water at a flow rate of 1.0 ml/min and the effluent was detected at 256 nm.

The HA concentration was determined by Total Organic Carbon (TOC) measurement using a Shimadzu V-570 TOC analyzer. To determine the HA concentration in the solutions spiked with both of the pollutants, the solution TOC and MP concentrations were measured. The mentioned concentrations were determined based on the results obtained from the HPLC chromatography in conjunction with the application of a calibration curve associated with the MP TOC to its measured concentration in the case of the MP contaminated solutions. The HA TOC of the solution was obtained by subtracting MP TOC from the solution TOC.

2.4. Batch adsorption experiments

To prepare the HA stock solution, 0.15 g of HA was dissolved in 1 L of D.I water at a proper pH in the solution. The mixture was then ultrasonicated for an hour. The supernatants were filtered through a 0.22 μm PTFE syringe filter to remove the undissolved HA particles and then, they were examined for HA concentration. The MP stock solution (200 mg/L) was prepared by dissolving 0.2 g MP in 1 L of D.I water. A series of 100-mL amber glass bottles containing 0.01 to 0.5 g of GAC per 50 ml of the solution were prepared. The stock solutions were added to each bottle and diluted with a predetermined amount of D.I water to provide 50-ml spiked solutions. The solution pH was adjusted from 4 to 10 using NaOH (0.1 M) and HCl (0.1 M) and measured using a pH meter (Orion Star Series, Thermo Electron, USA). All bottles were tightly sealed and incubated (immersed in a thermostatic bath) at $25 \pm 1^{\circ}$C and shaken at 100 rpm. The adsorbents were then separated through centrifugation at 8,000 rpm for 10 min. The concentrations of MP and HA at equilibrium were analyzed. The pollutants' adsorption capacity at equilibrium (q_e, mg/L) was calculated as follows [32]:

$$q_e = \frac{(C_0 - C_e)V}{M}, \tag{1}$$

where C_0 (mg/L) and C_e (mg/L) are the initial and equilibrium pollutant concentrations, respectively, V is the volume of the solution (L), and M is the mass of the adsorbents (g). These experiments are categorized into the following three sets in which the effects of the solution pH, GAC type and concentration, initial concentration of MP and HA on the equilibrium adsorption behavior of the pollutants were assessed:

1. Equilibrium monocomponent adsorption assessment of MP and HA from spiked solution onto the GACs;
2. Fractional equilibrium adsorption assessment of MP and HA from the spiked multicomponent solution onto the GACs, simultaneously. The initial concentrations of MP and HA were considered 30 ppm and 2.357 ppm TOC, respectively. This equilibrium set model concentration is addressed as a typical real condition;
3. Competitive equilibrium adsorption assessment at the same TOC concentrations (2.357 ppm) of MP and HA from spiked solution onto the GACs. The fractional adsorption potential of the pollutants was assessed to compare the effect of the pollutants' nature.

All of the experiments were independently run in duplicate at 25°C and pHs 5, 7, and 9. The results from the three assessments provided many insights into the MP adsorption mechanisms for aqueous solutions in the presence or absence of HA.

3. Results and discussion

3.1. Characterization of GACs

The respective BET surface areas of F400 and Norit GACs were 1034 and 682 m^2/g (Table 1). The total pore volume (0.53809 cm^3/g) and mesopore volume (0.18608 cm^3/g) of F400 GAC were higher than those of Norit GAC. The F400 GAC and Norit GAC had $V_{supermic}$ of 0.2246 and 0.1211 cm^3/g, respectively. The ultramicropore volumes were similar for both of the GACs.

Nitrogen adsorption-desorption isotherms at 77 K for GACs are given in Figure 1(a). The isotherms showed that F400 GAC had a greater nitrogen adsorption than the Norit GAC. The isotherms can be classified as I-H4 hybrid-type isotherms due to the hysteresis cycle characterization, which is associated

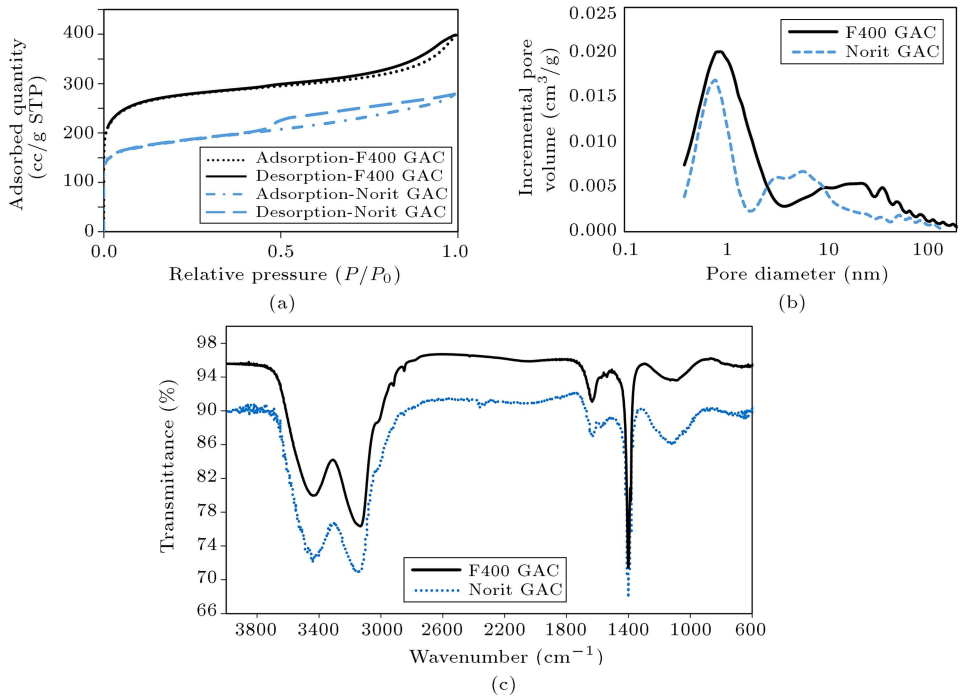

Figure 1. (a) N_2 adsorption-desorption isotherms at 77 K. (b) Pore size distributions obtained using the DFT method. (c) FTIR spectra of F400 and Norit GACs.

with capillary condensation inside mesopores and narrow slit pores in the micropore region. The pore size distribution plots of the GACs obtained from the DFT method are shown in Figure 1(b). The bimodal distribution related to an intensive peak for the micropores-ultramicropores and the broader range is associated with the mesoporosity of the materials.

The FT-IR spectra of GACs are presented in Figure 1(c). The two spectra exhibit a similar profile for carbonaceous materials. Two distinct broad and intense absorption bands for both F400 and Norit GACs at 3,440 and 3,140 cm^{-1} confirmed the presence of the hydroxyl (O-H) group. The absorption bands at 2,916 and 2,849 cm^{-1} indicate the asymmetric and symmetric C-H stretching vibrations of alkane groups -CH_3 and -CH_2 [33]. The absorption bands in the range of 1,536 to 1,634 cm^{-1} can be attributed to the C=C stretching vibration of the aromatic ring structures [34]. An intense peak appears for both GACs at 1,400 cm^{-1}, indicating the C-O and C=O bending absorption of carboxylic groups [35]. The bands in the range of 1,091 to 1,124 cm^{-1} correspond to the C-O stretching vibration of ether groups [36].

The surface morphology of F400 and Norit GACs was captured by SEM micrograph and the images are shown in Figure 2(a) and (b) and Figure 3(a) and (b), respectively. It is observed that S_{BET} of F400 GAC is higher than that of Norit GAC.

3.2. HA adsorption kinetics

A kinetic study was performed to assess the time required for achieving HA adsorption equilibrium. Figure 4(a) shows HA adsorption kinetics on F400 GAC. The kinetics experiment was performed at 0.004 g adsorbent/ml of solution and 2.357 mg/L HA initial concentration at a pH of 7 and a temperature of 25°C. Results indicate that equilibrium was achieved after two weeks. The Pseudo-First-Order (PFO) and Pseudo-Second-Order (PSO) kinetic models, by Eqs. (2) and (3), respectively, were applied to fit the HA adsorption kinetics data:

$$ln(q_e - q_t) = lnq_e - k_1 t, \tag{2}$$

$$\frac{t}{q_t} = \frac{1}{k_2 q_e^2} + \frac{1}{q_e} t, \tag{3}$$

where q_e is the equilibrium quantity of adsorption, q_t is the adsorption quantity at time t, and k_1 and k_2 are the apparent PFO and PSO rate constants, respectively. The PFO model was well fitted to the experimental results with a correlation coefficient of $R^2 = 0.9831$. This suggests that the adsorption process is diffusion controlled. The obtained value of q_e from the PFO model was 0.3614 mg g^{-1} and k_1 was 0.02152 h^{-1}. The R^2 value of the PSO kinetic model was 0.966. The PSO model constants of q_e and k_2 were 0.432 g $mg^{-1}h^{-1}$ and 0.05176 h^{-1}, respectively. The equilibrium adsorption times for MP onto both of the adsorbents were measured in less than three hours. The HA equilibrium adsorption times in the presence and/or absence of MP took two weeks for both of the GACs.

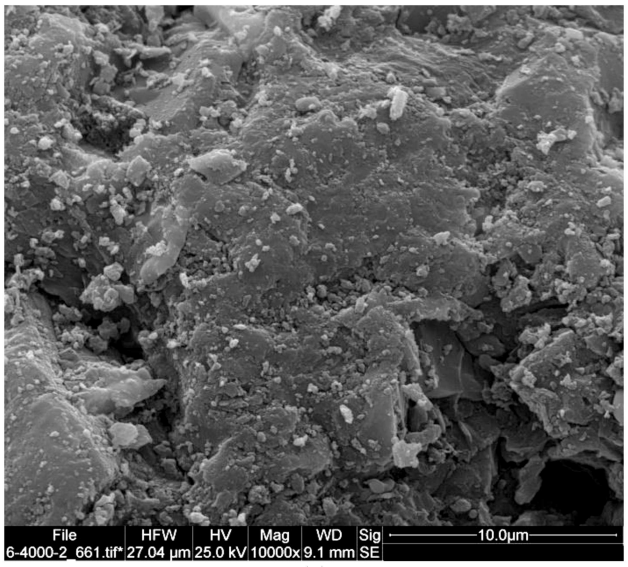

(a)

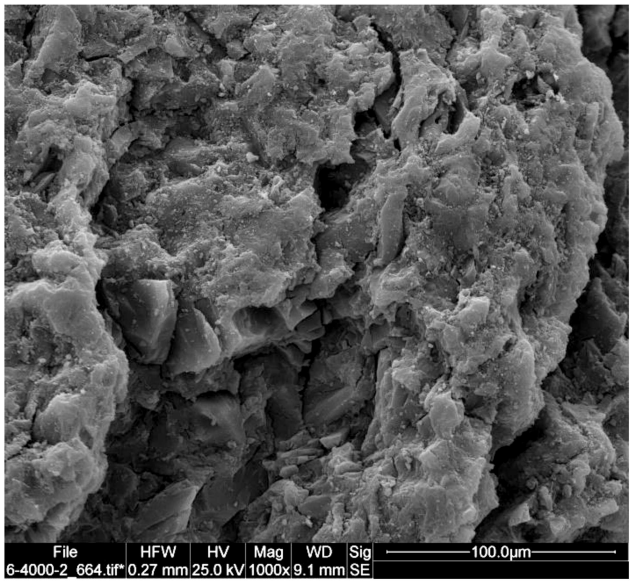

(b)

Figure 2. SEM micrographs of the surface from F400 GAC at (a) 10000× and (b) 1000× magnifications.

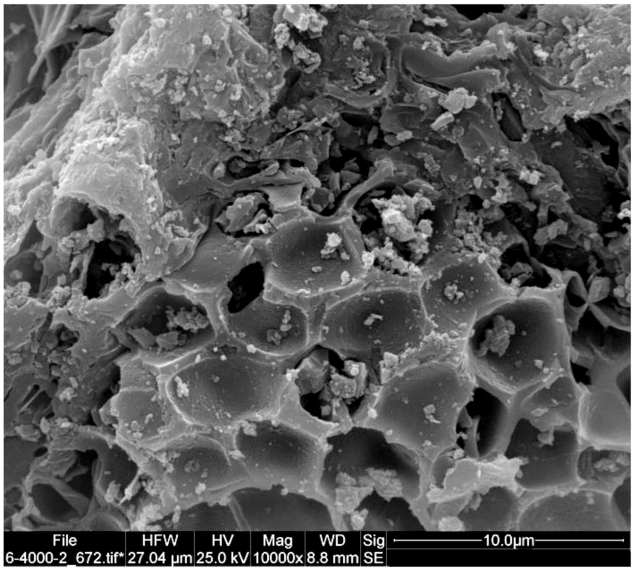

(a)

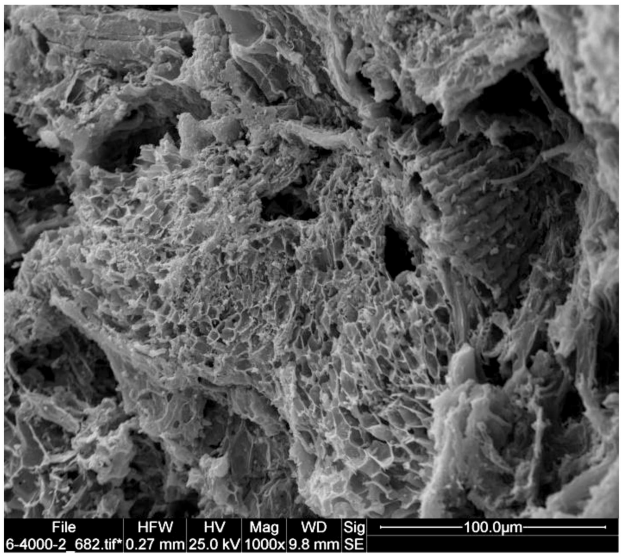

(b)

Figure 3. SEM micrographs of the surface from Norit GAC at (a) 10000× and (b) 1000× magnifications.

3.3. Adsorption isotherm

The adsorption results were fitted to the adsorbent dosage modified Freundlich model. Adsorbent dosage modified Freundlich isotherm [37] is an experimental model based on the hypothesis that layers of adsorbate form on an adsorbent heterogeneous surface. It takes into account the binding strength that reduces the site occupation through enhancement and is expressed by Eq. (4):

$$q_e = K\left(\frac{C_e}{M}\right)^{\left(\frac{1}{n}\right)}, \tag{4}$$

where K $(\mathrm{mg/g})(\mathrm{L/mg})^{1/n}$ and n are the Freundlich isotherm constants related to the adsorption capacity and adsorption intensity, respectively.

3.3.1. HA adsorption isotherm

The HA adsorption isotherms onto F400 and Norit GACs are presented in Figure 4(b) and (c), respectively. The concentration and adsorbed weights are expressed based on the TOC results. The modified Freundlich isotherm agrees with the HA adsorption results for both GACs at three different pH levels, indicating multilayer pollutant adsorption. By using the batch equilibrium method [38], the pHs for F400 and Norit GACs of the point-of-zero charges (pH_{pzc}) were measured at 7.8 and 8.4, respectively (Figure A.1). The GAC surface ionizable functional groups gain

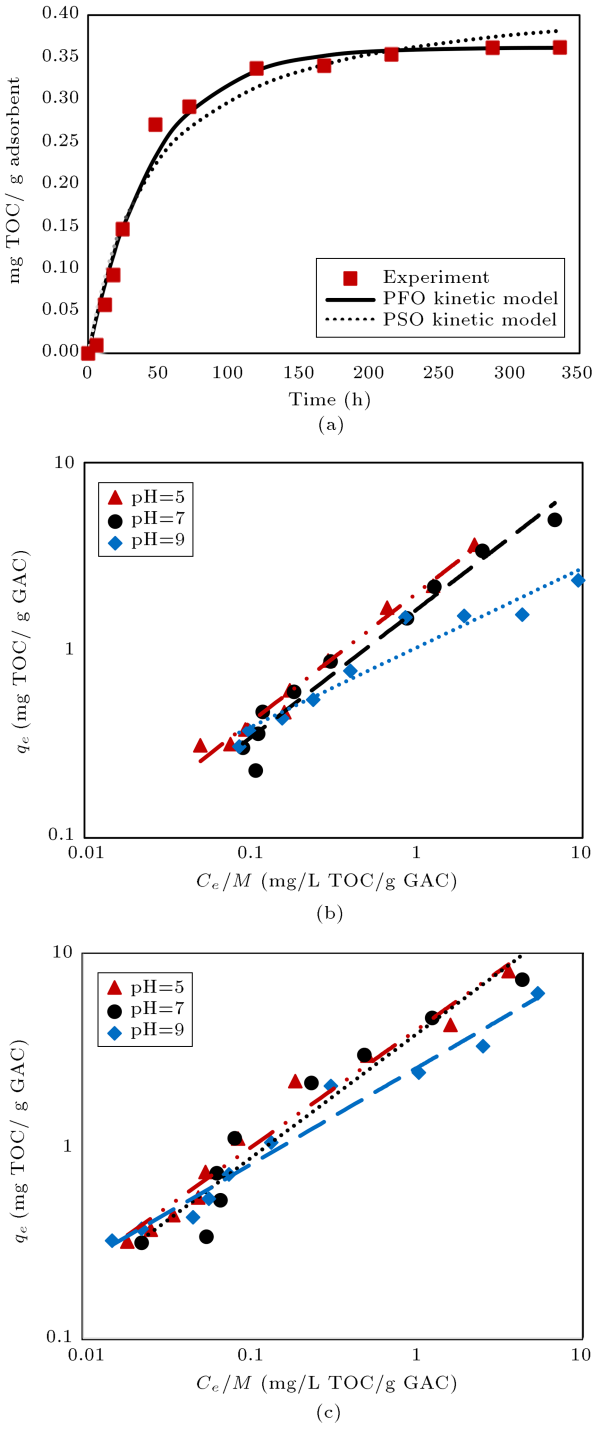

Figure 4. (a) HA adsorption kinetics onto the F400 GAC at 0.04 g of adsorbent/ml, HA initial TOC 2.357 ppm, pH 7, and 25°C. (b) Adsorption isotherms of HA onto the F400 GAC at pH 5, 7, and 9. (c) Adsorption isotherms of HA onto the Norit GAC at pH 5, 7, and 9.

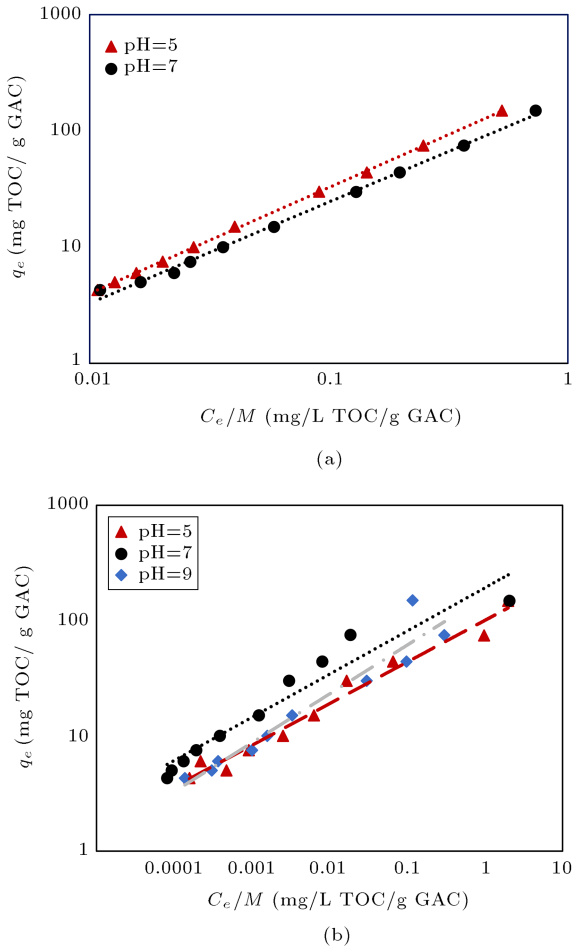

Figure 5. (a) MP adsorption isotherms onto the F400 GAC at pHs 5 and 7. (b) MP adsorption isotherms onto the Norit GAC at pHs 5, 7, and 9.

protons, and the surface becomes positively charged at an equilibrium pH less than pH_{pzc}. The GACs' surfaces exhibit negative charges when the solution pH is higher than pH_{pzc} [20]. The adsorption capacity of the Norit GAC was greater than that of F400 GAC. The pKa of the HA carboxylic group was less than 5. Thus, the HA's charge was negative in the pH range in this study [39]. The electrostatic attraction/repulsion mechanism between the GACs' surface and HA molecule charges could justify the adsorption results within the applied pH range [40]. Kołodziej et al. [41] argued that electrostatic attraction was mainly responsible for the twice higher degree of removal for two different HA fractions in the case of the modified ACs. The resulting trends are in accordance with the present findings. The adsorption capacity of HA on F400 GAC is in accordance with that reported in [37]. The values for the modified Freundlich model parameters for the three assessed category of adsorption experiments are tabulated in Table 2. High values of $1/n$ suggest a high affinity between the heterogeneous GAC sites and the pollutants.

3.3.2. MP adsorption isotherm

The MP adsorption isotherms at varying pHs on F400 and Norit GACs are presented in Figure 5(a) and (b), respectively. The behaviors of the isotherms are

Table 2. Adsorbent dosage modified Freundlich model parameters for the three studied adsorption categories.

Experiment	GAC Type/pollutant	Model parameters								
		pH=5			pH=7			pH=9		
		K	$1/n$	R^2	K	$1/n$	R^2	K	$1/n$	R^2
Monocomponent adsorption	F400/HA	2.012	0.6867	0.9921	1.6459	0.6819	0.9674	1.0329	0.4237	0.8946
	Norit/HA	3.9253	0.6109	0.9761	3.7277	0.6432	0.9449	2.4919	0.5003	0.9651
	F400/MP	264.73	0.9104	0.9998	181.16	0.8702	0.9977			
	Norit/MP	100.29	0.3614	0.9404	192.08	0.3746	0.8806	162.36	0.4238	0.5995
Simultaneous adsorption of MP and HA	F400/HA	1.3266	0.6894	0.9357	0.9702	0.7326	0.9907	1.5101	0.6211	0.9191
	F400/MP	233.96	0.8601	0.94	549.88	1.0282	0.9956	290.52	0.9016	0.9289
	Norit/HA	2.8517	0.6182	0.8373	2.2417	0.6765	0.9214	1.7866	0.6514	0.9957
Competitive adsorption of MP and HA	F400/HA	1.4536	0.6693	0.9831	1.4617	0.6343	0.9714	1.4253	0.6349	0.8685
	F400/MP	77.871	1.1069	0.9994	58.868	0.9443	0.988	109.55	1.0402	0.9886
	Norit/HA+MP	39.241	0.704	0.9639	32.229	0.7658	0.9846	27.21	0.7472	0.9986

described by the modified Freundlich model with a high correlation coefficient. The maximum adsorption capacity of MP on the GACs is in the order of the results achieved by Moreno-Marenco et al. [21] and Bernal et al. [22]; however, the physicochemical characteristics of their ACs and the experiment temperature were different than those in the present study.

The pollutant's hydrophobicity is a common mechanism in adsorption operation(s). The MP's octanol/water partition (log k_{ow}) logarithm is 1.96. Based on the hydrophobicity classification [42], the MP hydrophobicity was low; therefore, the hydrophobic mechanism was not a concern. In this study, the main MP adsorption mechanism for F400 GAC was hydrogen bonding. The adsorbent and adsorbate $-$OH functional group has the potential for hydrogen bonding. A decrease in pH enhances hydrogen bonding, while it weakens the π-π interaction. A schematic diagram of the MP adsorption mechanism on F400 GAC is presented in Figure 6.

The main mechanism for MP adsorption onto Norit GAC was the π-π type interaction. This adsorption process mechanism has already been reported in another work [43]. An increase in pH enhances the π-π interaction. The MP ionization percentage for a particular pH solution was calculated using Eq. (5) [44]:

$$Ionization\% = \frac{100}{1 + 10^{(pKa - \mathrm{pH})}}. \quad (5)$$

The MP molecular type was about 96% below pH 7. MP adsorption decreases beyond pH 7 when the MP ionization increases (see Table 3). The repulsive force and the ionized species intended to be less adsorbed on Norit GAC are responsible for the decrease in adsorption capacity. Bernal et al. [20] found that a commercial AC decreased the MP adsorption capacity due to the higher percentage of ionization and higher equilibrium pH than the adsorbent pH_{pzc}.

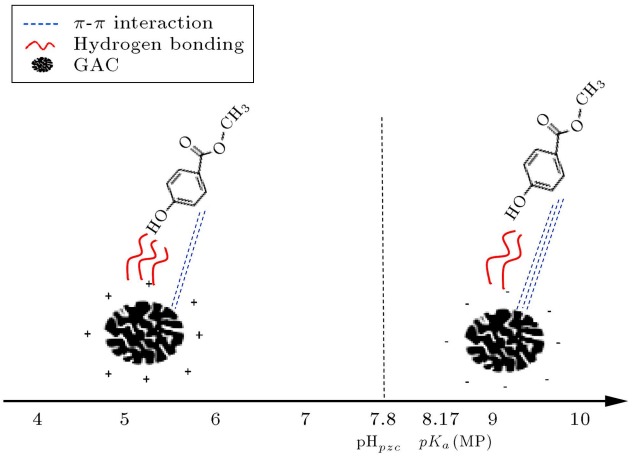

Figure 6. The schematic diagram of the MP adsorption mechanism on F400 GAC.

Table 3. MP hydrophobicity and percent ionization.

pH	Ionization (%)	$\log D$	$\log k_{oc} = \log D - 0.21$
5	0.03979	−1.44	−1.65
7	3.8287	0.543	0.333
9	79.92	1.263	1.053

3.4. Simultaneous adsorption of MP and HA

The simultaneous adsorption isotherms of MP and HA onto F400 GAC are presented in Figure 7(a) and (b).

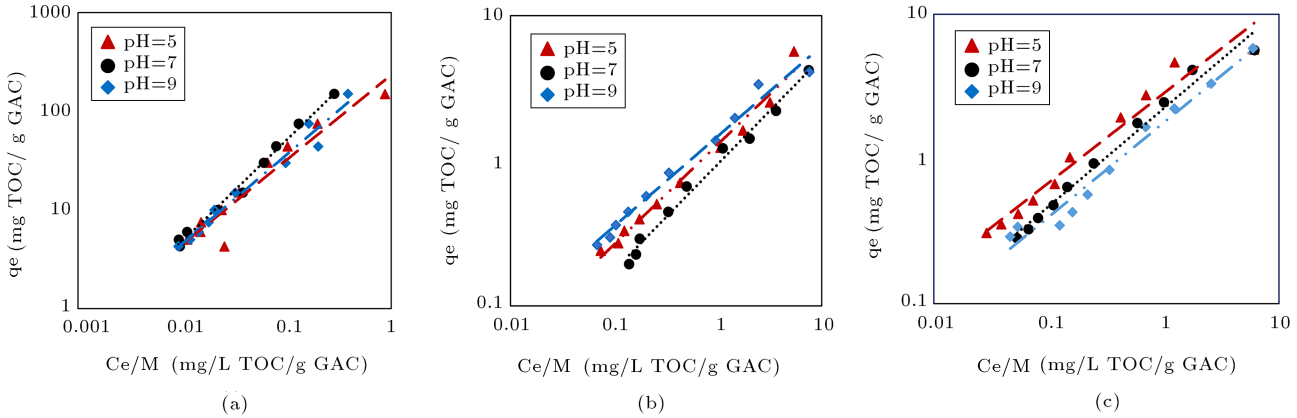

Figure 7. (a) MP adsorption isotherms onto F400 in the presence of HA at pHs 5, 7, and 9. (b) HA adsorption isotherms onto F400 in the presence of MP at pHs 5, 7, and 9. (c) HA adsorption isotherms onto Norit GAC in the presence of MP at pHs 5, 7, and 9.

The electrostatic force remains the main factor that justifies the pH effect on the adsorption results for F400 GAC, indicating a decrease in pH value and an increase in HA and MP adsorption. The MP deprotonates at a pH greater than pK_a 8.17, while it protonates at a pH lower than the pK_a value.

The GAC surface's repulsive electrostatic force of the maximum negative charge corresponds to the reduction of the HA adsorption capacity at pH 9. The GAC's available sites for MP adsorption were high at this pH and its capacity was higher than pH 7. The MP molecules were either directly adsorbed onto the GAC surface or indirectly adsorbed on already-adsorbed HA surface layers. HA's negative charge and MP's positive charge within the studied pH range showed that HA acted as a bridge between the GACs surface and MP molecules. It was expected that the MP adsorption capacity of the GACs under these conditions would be greater than that of aqueous systems which are contaminated only with MP.

The physicochemical properties of HA including the presence of different oxygen-containing functional groups, aromaticity, and hydrophobic interactions contributed to its aggregation extent. The presence of HA aggregates provides an additional hydrophobic domain for partitioning which enhances MP removal, although the steric blocking of GAC surfaces may inhibit its reduction to some extent [45]. The effect of GAC steric blocking was comparatively lower at the HA concentration in the present study.

In the presence of HA, a three-fold increase in MP adsorption at 1 mg/L TOC and pH 7 was observed. The average increase across all MPs in solution with a pH of 7 was approximately 2.2-fold. A similar behavior reported the HA effect on ciprofloxacin removal, which facilitated the adsorption process [46]. No significant increase in the MP adsorption capacity was observed under acidic conditions as a result of electrostatic repulsion force between HA and MP molecules at pH lower than 5. Delgado et al. [47] observed the significant presence of negative HA on ibuprofen and atenolol adsorption for two commercial GACs due to competition for adsorption sites and the pharmaceutically active compounds. The GAC's pore blockage was caused by HA, while Li et al. [30] claimed that HA was not effectively removed in competition with metaldehyde on a powdered activated carbon. Different HA effects on adsorption of ECs onto AC-type adsorbent could be attributed to different experimental conditions.

The MP's equilibrium adsorption onto Norit GAC in the presence of HA indicates that there does not exist any detectable MP at the liquid phase at pHs 5, 7, and 9 and all of the initial MP content has not been adsorbed. A comparison of these results and the MP adsorption results (Figure 5(b)) indicated that most of the MP molecules were adsorbed onto the HA molecules' surface. Although the initial HA molecule count was less than the MP molecule count, some HA molecules remained at the liquid phase in equilibrium conditions, while all of the MP molecules were adsorbed. The Norit GAC revealed a greater adsorption capacity for both of the HA and MP molecules than that for F400 GAC. The higher specific surface area and porosity properties of the F400 GAC cannot explain the behavior of these results. The HA adsorption isotherm onto the Norit GAC presented in Figure 7(c) was fitted to the modified Freundlich model. At pH less than 9, the MP molecules were protonated, which neutralized a part of the HA molecules' electron cloud and it led to the reduction of HA and GACs adsorption interactions. A schematic presentation of the MP adsorption mechanism on F400 GAC in the presence of HA is given in Figure 8.

3.5. Competitive adsorption of MP and HA

MP and HA competitive adsorption assessments were performed at the same TOC concentration. The MP and HA isotherms at varying pH values are presented

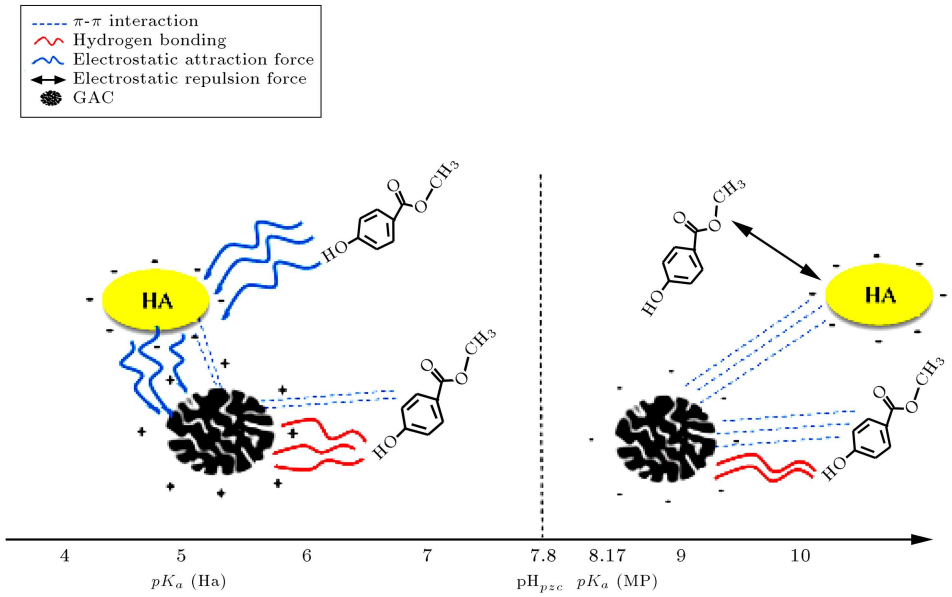

Figure 8. The schematic presentation of the MP adsorption mechanism on F400 GAC in the presence of HA.

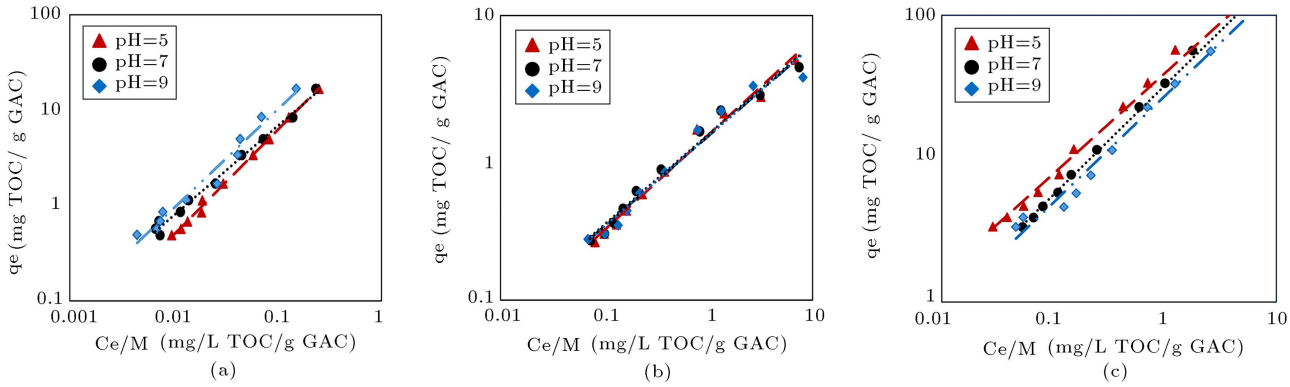

Figure 9. Competitive adsorption isotherms of (a) MP on F400 GAC in the presence of HA at pHs 5, 7, and 9. (b) HA on F400 GAC in the presence of MP at pHs 5, 7, and 9. and (c) overall adsorption isotherms of HA and MP on Norit GAC at pHs 5, 7, and 9.

in Figure 9(a) and (b). The results were fitted to the modified Freundlich isotherm model. In this experimental set, the MP concentrations for lower aggregates might become more significant [48] and lead to the formation of the weaker π-stacking interactions among the electrons in the MP aromatic rings, basic GAC functional groups, and the adsorption hydrophobicity. The organic carbon/water partition coefficient (k_{oc}) was applied to estimate the adsorbed MP values according to the Karickhoff empirical equation [49]:

$$\log k_{oc} = \log D - 0.21, \tag{6}$$

where $\log D$ is expressed through a modified criterion of the effect of pH on the $\log k_{ow}$. The explanation of the above relationship can be found in [50]. This criterion is defined as the equilibrium concentration ratio of the ionized and non-ionized forms of the pollutant at the octanol phase to the same species at the water phase. The MP percentage of hydrophobicity and ionization at the assessed pHs are tabulated in Table 3. The MP adsorption results were explained by the variation of k_{oc} with pH.

As depicted in Figure 9(b), HA's adsorption capacity onto the F400 GAC was the same in both of the competitive adsorption condition and different pH values. The number of specific affinity sites for the F400 GAC was high at low initial MP and HA concentrations.

No detectable amount of MP was measured in the solution in equilibrium conditions in the competitive adsorption experiment with Norit GAC. The amount of overall MP and HA adsorption onto the Norit GAC is shown in Figure 9(c). The MP molecules were protonated at pH less than 9, which neutralized a portion of the HA negative charges and reduced the

effect of the electron cloud between GAC and HA molecules. The HA adsorption increased as the pH decreased.

4. Conclusions

The adsorption of methylparaben (MP) and Humic Acid (HA) onto two commercial Granular Activated Carbons (GACs) was investigated in different pH aqueous solutions. The results indicated that the MP adsorption capacity onto both the F400 and Norit GACs was high (~ 150 mg/g). The main MP adsorption mechanism onto the F400 GAC was the hydrogen interaction between -OH functional groups from the MP molecules and the adsorbent. The fractional adsorption potential of the pollutants was assessed to compare the effects of the pollutants. The fractional adsorption capacity of MP and HA in a bicomponent solution was dependent on the pH of the solution and the initial concentrations of pollutants. The charge interactions among the molecules in the pollutants and the GAC surface were responsible for interpreting the complex adsorption behavior at different pHs. The MP adsorption capacity increased to nearly 2.2 fold in the presence of HA molecules and at a pH of 7 for both GACs. The experimental results were well fitted to the adsorbent dosage modified Freundlich isotherm. Both of the GACs have the potential to enhance the quality of drinking water from MP and HA contamination by applying a pre- or post- adsorption technique.

Acknowledgments

The authors wish to thank the Korea Institute of Energy Technology Evaluation and Planning (KETEP), Ministry of Trade, Industry, and Energy (MOTIE) of the South Korean government for supporting this research work (Grant No. 20182510102420).

References

1. Ryu, J., Oh, J., Snyder, S.A., et al. "Determination of micropollutants in combined sewer overflows and their removal in a wastewater treatment plant (Seoul, South Korea)", *Environ. Monit. Assess.*, **186**(5), pp. 3239–3251 (2014).
2. Luo, Y., Guo, W., Ngo, H.H., et al. "A review on the occurrence of micropollutants in the aquatic environment and their fate and removal during wastewater treatment", *Sci. Total Environ.*, **473**, pp. 619–640 (2014).
3. Carmalin, S.A. and Lima, E.C. "Removal of emerging contaminants from the environment by adsorption", *Ecotox. Environ. Saf.*, **150**, pp. 1–17 (2018).
4. Lincho, J., Martins, R.C., and Gomes, J. "Paraben compounds-part I: An overview of their characteristics, detection, and impacts", *Appl. Sci.*, **11**(5), pp. 2307(1–37) (2021).
5. Gonzalez-Marino, I., Quintana, J.B., Rodriguez, I., et al. "Evaluation of the occurrence and biodegradation of parabens and halogenated by-products in wastewater by accurate-mass liquid chromatography-quadrupole-time-of-flight-ma ss spectrometry (LC-QTOF-MS)", *Water Res.*, **45**(20), pp. 6770–6780 (2011).
6. Blédzka, D., Gromadzińska, J., and Wásowicz, W. "Review parabens. From environmental studies to human health", *Environ. Int.*, **67**, pp. 27–42 (2014).
7. Rasheed, T., Bilal, M., Nabeel, F., et al. "Environmentally-related contaminants of high concern: Potential sources and analytical modalities for detection, quantification, and treatment", *Environ. Int.*, **122**, pp. 52–66 (2019).
8. Brausch, J.M. and Rand, G.M. "A review of personal care products in the aquatic environment: Environmental concentrations and toxicity", *Chemosphere*, **82**(11), pp. 1518–1532 (2011).
9. Li, W., Gao, L., Shi, Y., et al. "Spatial distribution, temporal variation and risks of parabens and their chlorinated derivatives in urbane surface water in Beijing, China", *Sci. Total Environ.*, **539**, pp. 262–270 (2016).
10. Pycke, B.F.G., Geer, L.A., Dalloul, M., et al. "Maternal and fetal exposure to parabens in a multiethnic urban U.S. population", *Environ. Int.*, **84**, pp. 193–200 (2015).
11. Molins-Delgado, D., Diaz-Cruz, M.S., and Barcelo, D. "Ecological risk assessment associated to the removal of endocrine-disrupting parabens and benzophenone-4 in wastewater treatment", *J. Hazard. Mater.*, **310**, pp. 143–151 (2016).
12. Haman, C., Dauchy, X., Rosin, C., et al. "Occurrence, fate and behavior of parabens in aquatic environments: A review", *Water Res.*, **68**, pp. 1–11 (2015).
13. Liao, C., Lee, S., Moon, H.B., et al. "Parabens in sediment and sewage sludge from the United States, Japan, and Korea: spatial distribution and temporal trends", *Environ. Sci. Technol.*, **47**(19), pp. 10895–10902 (2013).
14. Gorga, M., Petrovic, M., and Barcelo, D. "Multi-residue analytical method for the determination of endocrine disruptors and related compounds in river and wastewater using dual column liquid chromatography switching system coupled to mass spectrometry", *J. Chromatogr. A.*, **1295**, pp. 57–66 (2013).
15. Yamamoto, H., Tamura, I., Hirata, Y., et al. "Aquatic toxicity and ecological risk assessment of seven parabens: individual and additive approach", *Sci. Total Environ.*, **410**, pp. 102–111 (2011).
16. Cela, R., Gonzalez, I., Quintana, J.B., et al. "Occurrence and biodegradation of parabens and their most common halogenated by-products in wastewater", *Int Symp Environ. Anal. Chem.*, Rome (2010).

17. Tay, K.S., Rahman, N.A., and Abas, M.R.B. "Ozonation of parabons in aqueous solution: Kinetics and mechanism of degradation", *Chemosphere*, **81**(11), pp. 1446–1453 (2010).

18. Ping, C.Y. "Adsorption of parabens in aqueous solution onto β-cyclodextrin cross-linked polymer", MSC Dissertation, University of Malaya, Kuala Lumpur (2013).

19. Mohammadi, F., Esrafili, A., Sobhi, H.R., et al. "Evaluation of adsorption and removal of methylparaben from aqueous solutions using amino-functionalized magnetic nanoparticles as an efficient adsorbent: Optimization and modeling by response surface methodology (RSM)", *Desalin. Water Treat.*, **103**, pp. 248–260 (2018).

20. Bernal, V., Giraldo, L., Moreno-Piraján, J.C., et al. "Mechanisms of methylparaben adsorption onto activated carbons: Removal tests supported by a calorimetric study of the adsorbent-adsorbate interactions", *Molecules*, **24**(3), p. 413 (2019).

21. Moreno-Marenco, A.R., Giraldo, L., and Moreno-Pirajan, J.C. "Parabens adsorption onto activated carbon: Relation with chemical and structural properties", *Molecules*, **24**(23), p. 4313 (2019).

22. Bernal, V., Giraldo, L., and Moreno-Pirajan, J.C. "Physicochemical parameters of the methylparaben adsorption onto activated carbon and their relationship with the surface chemistry", *ACS Omega*, **6**(13), pp. 8797–8807 (2021).

23. Bueno, M.H., Boluda-Botella, N., and Rico, D.P. "Removal of emerging pollutants in water treatment plants: adsorption of methyl and propylparaben onto powdered activated carbon", *Adsorption*, **25**, pp. 983–999 (2019).

24. Magdaleno, G.B. and Coichev, N. "Chemiluminescent determination of humic substances based on the oxidation by peroxymonosulfate", *Anal. Chim. Acta*, **552**(1–2), pp. 141–146 (2005).

25. Zimmer, G., Brauch, H.J., and Sontheimer, H. "Activated-carbon adsorption of organic pollutants aquatic humic substances", *Chapter 33. Adv. Chem.*, **219**, pp. 579–596 (1989).

26. Bhatnagar, A. and Sillanpää, M. "Removal of Natural Organic Matter (NOM) and its constituents from water by adsorption - A review", *Chemosphere*, **166**, pp. 497–510 (2017).

27. Gao, Y. and Deshusses, M.A. "Adsorption of clofibric acid and ketoprofen onto powdered activated carbon: Effect of natural organic matter", *Environ. Technol.*, **32**(15), pp. 1719–1727 (2011).

28. Behera, S.K., Oh, S.Y., and Park, H.S. "Sorption of triclosan onto activated carbon, kaolinite and montmorillonite: effects of pH, ionic strength, and humic acid", *J. Hazard. Mater.*, **179**(1–3), pp. 684–691 (2010).

29. Zhang, S.J., Shao, T., and Karanfil, T. "The effects of dissolved natural organic matter on the adsorption of synthetic organic chemicals by activated carbons and carbon nanotubes", *Water Res.*, **45**(3), pp. 1378–1386 (2011).

30. Li, Z., Yang, Y., Jáuregui-Haza, U., et al. "The impact of humic acid on metaldehyde adsorption onto powdered activated carbon in aqueous solution", *RSC Adv.*, **9**, pp. 11–22 (2019).

31. Rivera-Utrilla, J., Bautista-Toledo, I., Ferro-Garcia, M.A., et al. "Activated carbon surface modifications by adsorption of bacteria and their effect on aqueous lead adsorption", *J. Chem. Technol. Biotechnol.*, **76**, pp. 1209–1215 (2001).

32. Jokar Baloochi, Sh., Solaimany Nazar, A.R., Farhadian, M., et al. "2.4-dichlorophenoxyacetic acid adsorption from contaminated water through activated carbon reclaimed with zero-valent iron and titanium dioxide", *Sci. Iran.*, **25**(3), pp. 1395–1411 (2018).

33. Tyagi, A., Das, S., and Srivastava, V.C. "Removal of toxic hydroquinone: Comparative studies on use of iron impregnated granular activated carbon as an adsorbent and catalyst", *Environ. Eng. Res.*, **24**(3), pp. 474–483 (2019).

34. Osman, A.I., Farrell, C., Al-Muhtaseb, A.H., et al. "The production and application of carbon nanomaterials from high alkali silicate herbaceous biomass", *Sci. Rep.*, **10**, 2563 (2020).

35. Ioannou, Z. and Simitzis, J. "Adsorption of methylene blue dye onto activated carbons based on agricultural by products: equilibrium and kinetic studies", *Water Sci. Technol.*, **67**(8), pp. 1688–1694 (2013).

36. Singh, R., Kumar, M., Khajuria, H., et al. "Solvothermal synthesis of ZnO-nitrogen doped graphene composite and its application as catalyst for photodegradation of organic dye methylene blue", *Acta. Chim. Slov.*, **65**(2), pp. 319–327 (2018).

37. Yan, L., Fitzgerald, M., Khov, C., et al. "Elucidating the role of phenolic compound in the effectiveness of DOM adsorption on novel tailored activated carbon", *J. Hazard. Mater.*, **262**, pp. 100–105 (2013).

38. Iida, T., Amano, Y., Machida, M., et al. "Effect of surface property of activated carbon on adsorption of nitrate ion", *Chem. Pharm. Bull.*, **61**(11), pp. 1173–1177 (2013).

39. Kilduff, J., Karanfil, T., and Weber, W. "Competitive interactions among components of humic acids in granular activated carbon adsorption systems: Effects of solution chemistry", *Environ. Sci. Technol.*, **30**, pp. 1344–1351 (1996).

40. Yan, X., Du, W., Ma, C., et al. "Humic acid adsorption behavior and mechanism comparison between biochars and activated carbon", *Desalin. Water Treat.*, **173**, pp. 213–222 (2020).

41. Kołodziej, A., Fuentes, M., Baigorri, R., et al. "Mechanism of adsorption of different humic acid fractions on mesoporous activated carbons with basic surface characteristics", *Adsorpt.*, **20**, pp. 667–675 (2014).

42. Nam, S.-W., Choi, D.-J., Kim, S.-K., et al. "Adsorption characteristics of selected hydrophilic and hydrophobic micropollutants in water using activated carbon", *J. Hazard. Mater.*, **270**, pp. 144–152 (2014).
43. Cotoruelo, L.M., Marques, M.D., Levia, A., et al. "Adsorption of oxygen-containing aromatics used in petrochemical, pharmaceutical, and food industries by means of lignin based active carbons", *Adsorpt. J. Int. Adsorpt. Soc.*, **17**, pp. 539–550 (2011).
44. Iovino, P., Canzano, S., Capasso, S., et al. "A modeling analysis for the assessment of ibuprofen adsorption mechanism onto activated carbons", *Chem. Eng. J.*, **277**, pp. 360–367 (2015).
45. Yu, S., Liu, J., Yin, Y., et al. "Interactions between engineered nanoparticles and dissolved organic matter: A review on mechanisms and environmental effects", *J. Environ. Sci.*, **63**, pp. 198–217 (2018).
46. Wang, W., Cheng, J., Zhou, Q., et al. "Effect of humic acid on ciprofloxacin removal by magnetic multifunctional resins", *Sci. Rep.*, **6**, 30331 (2016).
47. Delgado, L.F., Charles, P., Glucina, K., et al. "Adsorption of ibuprofen and atenolol at trace concentration on activated carbon", *Sep. Sci. Technol.*, **50**(10), pp. 1487–1496 (2015).
48. Shetty, A.S., Zhang, J., and Moore, J.S. "Aromatic π-stacking in solution as revealed through the aggregation of phenylacetylene macrocycles", *J. Ame. Chem. Soc.*, **118**(5), pp. 1019–1027 (1996).
49. Karickhoff, S.W., Brown, D.S., and Scott, T.A. "Sorption of hydrophobic pollutants on natural sediments", *Water Res.*, **13**(3), pp. 241–248 (1979).
50. Schwarzenbach, R., Geschwend, P., and Imboden, D., *Environmental Organic Chemistry*, John Wiley & Sons (2003).

Appendix A

The results of pH_{pzc} measurement of the studied GACs through the pH drift method are presented in Figure A.1.

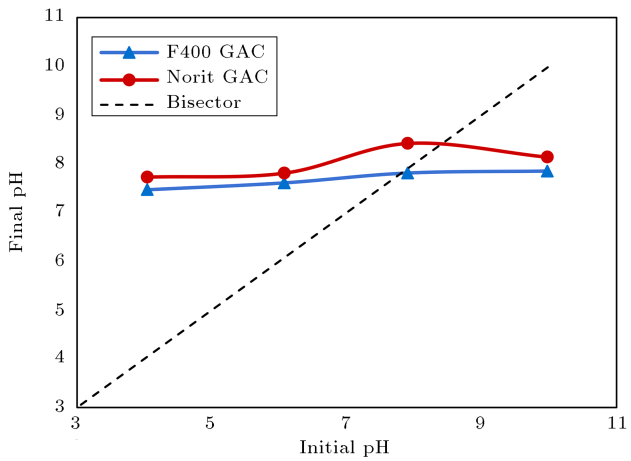

Figure A.1. The pH_{pzc} results of the studied GACs.

Biographies

Ali Reza Solaimany Nazar is currently an Associate Professor at the Chemical Engineering Department at the University of Isfahan, Iran. He received his PhD in Chemical Engineering from Amirkabir University of Technology, Iran. His current research interests are mainly in the application of nanomaterials to oil flow, convection heat transfer, and water and wastewater treatment fields. His specific research topic is emerging organic compounds removal from the aqueous phase using adsorption technique and advanced oxidation process. He has published 100 research articles in well-known peer-reviewed scientific journals.

Mayur Bharat Kurade has acquired his PhD at Shivaji University, Kolhapur, India and is currently working as a Research Associate Professor at the Department of Earth Resources and Environmental Engineering, Hanyang University, Seoul, South Korea. He has demonstrated experience in the field of bioenergy generation with specialization in biofuels production, anaerobic digestion of waste organic resources, mass cultivation of the 3rd generation biomass, and its pretreatment and fermentation technologies. His specific interests include biological wastewater treatment, sludge treatment, organic waste management, and emerging organic compounds removal from wastewater. The developed technologies with an integrated approach to wastewater treatment and bioenergy generation have aimed at 'zero waste biofuel generation.' Dr. Kurade has published 80 research articles in well-known peer-reviewed international journals of high repute along with 3 book chapters and 1 patent focusing on wastewater pollution control technologies.

Moonis Ali Khan received his PhD in Applied Chemistry from Aligarh Muslim University, Aligarh, India, in 2009. From the year 2009 to 2011, he worked as a Post-Doctoral Researcher at Yonsei University, South Korea, and University Putra Malaysia, Malaysia. In 2011, he joined the Chemistry Department at the King Saud University (KSU), Saudi Arabia as an Assistant Professor. Currently, he is working as an Associate Professor at KSU. He is an interfacial chemist and his research is focused on the synthesis and development of novel materials for energy and environmental remediation applications. To date, he has guided two doctoral students for their respective degrees. He has published more than a hundred (research and review) articles and has two U.S. patents to his credit.

Byong-Hun Jeon is a Professor at the Department of Earth Resources and Environmental Engineering at Hanyang University, South Korea. He holds a

BSc degree in Mineral and Petroleum Engineering from Hanyang University as well as MSc and PhD degrees in Civil and Environmental Engineering from Pennsylvania State University, USA. His current research interests include environmental biotechnology, bioremediation, anaerobic digestion, fermentation, and environmental biogeochemistry. His research group is primarily working on organic waste management through bioenergy production and soil and water pollution control using biological and chemical tools. His current specific emphasis has been on the meta-omics studies of the environmental microbiota using state-of-the-art high-throughput sequencing methods. His in-depth research on these topics has yielded more than 300 research articles in well-known, international peer-reviewed journals. Some of his highlighted research works have appeared in Nature Communications, Energy and Environmental Sciences, Coordination Chemistry Reviews, Trends in Biotechnology, and Progress in Energy Combustion Science.